Peptides 32 (2011) 1–10

Contents lists available at ScienceDirect

Peptides

journal homepage: www.elsevier.com/locate/peptides

# The *Mycobacterium tuberculosis* membrane protein Rv0180c: Evaluation of peptide sequences implicated in mycobacterial invasion of two human cell lines

Silvia Marcela Cáceres[a], Marisol Ocampo[a,b,*], Gabriela Arévalo-Pinzón[a,b], Ronald Andrés Jimenez[a,b], Manuel Elkin Patarroyo[a,c], Manuel Alfonso Patarroyo[a,b]

[a] *Fundación Instituto de Inmunología de Colombia (FIDIC), Bogotá, Colombia*
[b] *Universidad del Rosario, Bogotá, Colombia*
[c] *Universidad Nacional, Bogotá, Colombia*

ARTICLE INFO

*Article history:*
Received 28 July 2010
Received in revised form
21 September 2010
Accepted 21 September 2010
Available online 29 September 2010

*Keywords:*
Rv0180c
*Mycobacterium tuberculosis*
Invasion inhibition assays
PEXEL motif
Latex bead internalization

ABSTRACT

The identification and characterization of hypothetical membrane proteins from *Mycobacterium tuberculosis* have led to a better understanding of the mechanisms used by this pathogen to invade and survive inside host cells. This study assessed the presence, transcription, localization and possible biological activity of the conserved hypothetical protein Rv0180c from *M. tuberculosis*. Bioinformatics analyses indicated that Rv0180c contains a signal peptide, six possible transmembrane helices and a *Plasmodium* Export Element (PEXEL)-like motif. PCR analyses showed the presence of the *Rv0180c* gene in strains from the *M. tuberculosis* complex; but transcription was not detected in *Mycobacterium microti*. Sera against synthetic peptides of Rv0180c recognized two protein bands in *M. tuberculosis* H37Rv sonicate: a ~48-kDa band close to the predicted molecular mass of Rv0180c (47.6 kDa), and a 63-kDa band probably caused by protein modifications. Moreover, the same sera located the protein on the surface of *M. tuberculosis* H37Rv bacilli by immunoelectron microscopy. Twenty-three synthetic peptides spanning the entire length of Rv0180c were tested for their ability to bind to U937 and A549 cells, finding nine high-activity binding peptides (HABPs) specific for both cell types, two HABPs specific for A549 cells (namely 31032 and 31044) and two HABPs specific for U937 cells (namely 31025 and 31041). HABPs inhibited invasion of *M. tuberculosis* H37Rv into A549 or U937 cells by significant percentages and facilitated internalization of latex beads in A549 cells. The Rv0180c HABPs herein reported could be preliminary candidates to be assessed as components of a multiepitope, chemically synthesized, subunit-based vaccine against tuberculosis.


## 1. Introduction

Tuberculosis (TB) is a major cause of illness and death worldwide. It is estimated that TB caused around 9.27 million new cases and 1.3 million deaths in 2007, with HIV-positive people being one of the most severely affected populations with an estimate of two million deaths [76]. Up to date, the directly observed treatment-short course (DOTS) strategy recommended by the World Health Organization (WHO) has efficiently detected and treated TB by using a combination of three antibiotics to avoid the emergence of drug-resistance strains, but unfortunately its high cost has limited an efficient implementation of this strategy [78]. Additionally, the protective efficacy of the Bacillus Calmette-Guérin (BCG) vaccine against pulmonary TB, the most common form of the disease, varies considerably in adults, which further stresses the importance of developing more effective prevention and control measures [66].

*Mycobacterium tuberculosis*, the main causative agent of TB, secretes high amounts of proteins and complex lipids that form a structure known as the mycobacterial cell envelope, which protects mycobacteria and plays an active role in cell–cell interactions, cell signaling and protein transport, among other functions [6,7,16,27,73]. In addition, a large number of surface and secreted mycobacterial proteins are known to be important for replication and survival of mycobacteria inside the host macrophage, and have been implicated in the modulation of the host's immune response [20,36]. For this reason, most search for new vaccine targets has focused on screening the genomic sequence of *M. tuberculosis* H37Rv [14] for mycobacterial proteins and lipids that are exposed on the cell surface or that are secreted either to the extra-

*Abbreviations:* A549, carcinomic human type II alveolar epithelial cells; TB, tuberculosis; DOTS, directly observed treatment short-course; IEM, immunoelectron microscopy; PEXEL, *Plasmodium* Export Element; HABP, high-activity binding peptide; HCT, host cell targeting signal; MOTT, mycobacteria other than tuberculosis; MTBC, *Mycobacterium tuberculosis* complex; U937, monocyte-derived macrophages.

* Corresponding author at: Carrera 50 # 26-20, Bogotá, Colombia.
Tel.: +57 1 481 5219/324 4672x137; fax: +57 1 481 5269.
*E-mail address:* marisol.ocampo@urosario.edu.co (M. Ocampo).

0196-9781/$ – see front matter © 2010 Elsevier Inc. All rights reserved.
doi:10.1016/j.peptides.2010.09.017

cellular milieu or to subcellular compartments within infected macrophages [6,7,79,80].

Rv0180c is a probable conserved transmembrane protein of unknown function that shares high sequence similarity with putative conserved membrane and transmembrane proteins from different mycobacterial species. Moreover, bioinformatics analyses of the Rv0180c sequence showed the presence of a functional Rx[LI]x[DEQ]-like motif, which is also found in proteins of some virulent mycobacterial species. This conserved motif is known as the *Plasmodium* Export Element (PEXEL) or Host Cell-Targeting Signal (HCT) and is formed by five amino acids as follows: a hydrophobic amino acid (Arg) at position 1, a hydrophobic amino acid at position 3 (Leu or Ile), another less conserved amino acid at position 5 (mainly Asp, Glu or Gln), and non-charged amino acids at positions 2 and 4. In the protozoan *Plasmodium* spp., an obligate intracellular parasite that invades and replicates inside erythrocytes in which over 400 parasite proteins are translocated across the outer parasitophorous vacuole membrane into the host erythrocyte cytosol [60], the PEXEL motif is hypothesized to conform a signal mediator of this important protein trafficking [34,47]. A similar but shorter motif (RxLR) has been also identified in four virulent Oomycete Avr proteins from the phytopathogens *Phytophthora sojae*, *Phytophthora infestans* and *Hyaloperonospora parasitica* [2,5,56,61], in which the motif has been suggested to be involved in secretion and targeting of the protein effectors delivered from the haustoria to the plant cells, although it does not appear to be related to the activity of such effectors [9,10].

The aim of this study was to assess the presence of the *Rv0180c* gene, and the transcription and possible localization of the protein product in mycobacterial surface through the use of molecular biology tools and immunoelectron microscopy (IEM). The entire sequence of Rv0180c was synthesized as 20-mer non-overlapping synthetic peptides and analyzed in binding assays with human type II A549 alveolar epithelial cells and macrophages derived from U937 monocytes seeking to identify high-activity binding peptides (HABPs). The ability of HABPs to inhibit invasion of *M. tuberculosis* H37Rv and facilitate internalization of latex beads was examined in order to identify Rv0180c HABPs that could be use in the design of a multiepitope, chemically synthesized subunit-based antituberculous vaccine.

## 2. Material and methods

### 2.1. Bioinformatics analyses

The sequence of the *M. tuberculosis* Rv0180c protein was retrieved from the Tuberculist Webserver available at http://genolist.pasteur.fr/TubercuList/. Protein alignments and homologies were obtained using BLAST (http://www.ncbi.nlm.nih.gov/BLAST/) [1]. Protein features and GRAVY scores were calculated using PROTPARAM (http://us.expasy.org/tools/protparam.html) [43]. The signal sequence prediction was obtained using SignalP 3.0 (http://www.cbs.dtu.dk/services/SignalP) [8]. Transmembrane helices were predicted using TMHMM server v.2.0 (http://www.cbs.dtu.dk/services/TMHMM/) [41,64]. Additionally, the SOPMA server was inquired to analyze the secondary structure of Rv0180c (http://npsa–pbil.ibcp.fr/cgi–bin/npsa_automat.pl?page=npsa_sopma.html) [32]. Protein motifs were identified using the Scanprosite tool (http://www.expasy.org/tools/scanprosite/) [22].

### 2.2. Mycobacterial strains and culture

The American Type Culture Collection (ATCC) was the source of the following mycobacterial strains: *Mycobacterium tuberculosis* H37Rv (ATCC 27294), *Mycobacterium tuberculosis* H37Ra (ATCC 25177), *Mycobacterium bovis* (ATCC BAA-935), *Mycobacterium bovis* BCG (ATCC 35734, Pasteur substrain), *Mycobacterium africanum* (ATCC 25420), *Mycobacterium flavescens* (ATCC 14474), *Mycobacterium fortuitum* (ATCC 6841), *Mycobacterium szulgai* (ATCC 65799), *Mycobacterium peregrinum* (ATCC 14467), *Mycobacterium phlei* (ATCC 11758), *Mycobacterium scrofulaceum* (ATCC 19981), *Mycobacterium avium* (ATCC 25291). *Mycobacterium microti* (Pasteur strain) was kindly provided by Dr. F. Portaels form the Institute of Tropical Medicine, Belgium. Mycobacteria were grown in 7H9 (Difco) supplemented with albumin, dextrose, NaCl (ADC) and incubated at their optimum temperature until cultures have reached an $OD_{600}$ of 0.5–1.0.

### 2.3. Extraction of genomic DNA and PCR amplification

The DNA was extracted from mycobacterial cultures using the UltraClean™ Microbial DNA Isolation Kit according to the manufacturer's instructions (MO BIO Laboratories Inc., Carlsbad, CA). The *Rv0180c* gene was amplified on a Perkin–Elmer thermal cycler Gene Amp PCR system 9600 using the amplification primers E11-F (3′-GCACCCAACCCCAAGCG-5′) and E12-R (5′-CCCCGAAGTCCCGTAGC-3′). PCR reactions were performed in 10 μL final volumes containing: 1 μL gDNA, 1U *Taq* polymerase (Promega), 1× *Taq* polymerase reaction buffer, 1.5 mM $MgCl_2$, 0.2 mM dNTPs and 0.4 μM of each primer. PCR conditions were as follows: initial DNA denaturing for 5 min at 94 °C, followed by 30 cycles of 1 min annealing at 59 °C, 45 s extension at 72 °C and 1 min denaturing at 94 °C. A final 5 min extension cycle was performed at 72 °C. Amplification products were separated by electrophoresis on 1% agarose gels stained with SYBR safe (Invitrogen, Eugene, Oregon). A 1-kb DNA ladder was loaded in each gel for size reference (Gibco).

### 2.4. RNA isolation and RT-PCR assays

The total RNA was extracted from mycobacterial cultures by adding Trizol (Invitrogen, Carlsbad, CA) and then precipitating the RNA with isopropanol. The precipitated RNA was washed with 70% ethanol, suspended in DEPC-treated water and quantified using a GeneQuant spectrophotometer (Pharmacia Biotech, Piscataway, NJ). It was then treated with DNAse I (Invitrogen, Carlsbad, CA) and used as template for the RT-PCR assays. cDNA synthesis was performed according to the SuperScript III First strand synthesis system for RT-PCR (Invitrogen, Carlsbad, CA), following the manufacturer's instructions. The *rpo*-B gene was used as positive transcription control (forward 3′-TCAAGGAGAAGCGCTACGA-5′ and reverse 5′-GGATGTTGATCAGGGTCTGC-3′ primers). *M. tuberculosis* H37Rv treated with DNAse I was used as negative control for cDNA synthesis.

### 2.5. Cell cultures

The U937 (ATCC CRL-1593.2) and A549 (ATCC CCL-185) cell lines were cultured in RPMI 1640 supplemented with 10% heat-inactivated fetal bovine serum (Hyclone, Logon, UT), at 37 °C and under a 5% $CO_2$ atmosphere. Cells were dislodged using cell dissociation solution non-enzymatic 1× (Sigma), collected and washed with PBS before being used.

### 2.6. Peptide synthesis and radiolabeling

A total of 23 peptides were synthesized according to the multiple solid phase methodology [37]. These peptides were 20 amino acids in length and spanned the entire sequence of Rv0180c without overlapping. One Tyrosine was added to the C-terminus of

those peptides lacking this residue in their sequences to enable $^{125}$I-radiolabeling [68,81]. RP-HPLC-purified peptides were radiolabeled according to previously described techniques [26,70,81]. Briefly, chloramine-T (0.3 μmol) and Na$^{125}$I (3.2 μL, 100mCi/mL; MB Biomedicals) were added to a 5 μL peptide solution (1 μg/μL). The solution was then incubated for 15 min at 18 °C and added sodium metabisulfite (0.18 μmol). Radio-labeled peptides were then purified on a Sephadex G-10 packed column (Pharmacia, Uppsala, Sweden).

### 2.7. Binding and saturation assays

A549 and U937 cells ($1.5 \times 10^6$ cells) were incubated for 90 min at 4 °C with increasing concentrations of radio-labeled peptide (0–950 nM) in the presence or absence of unlabeled peptide (40 μM). The reaction mixture was passed through a 60:40 dioctylphthalate-dibutylphthalate cushion and spun at $4500 \times g$ for 3 min. Cell-associated radioactivity was quantified in a gamma counter (Gamma Counter Cobra II, Packard Instrument Co., Meriden, CT, USA). Specific binding activity values were obtained by determining the difference between total and non-specific binding. Peptides showing a specific binding activity of ≥1% were considered HABPs, according to previously described criteria [26,29,53].

For saturation assays, macrophages derived from U937 monocytes ($1.5 \times 10^6$ cells) were incubated with 0–3500 nM concentrations of radio-labeled HABPs in the presence or absence of unlabeled peptide (30 μM). The obtained plots were analyzed by saturation and Hill analyses [38,74,81].

### 2.8. Immunization of animals

Two goats previously determined to be non-reactive to *M. tuberculosis*, as determined by Western blotting of *M. tuberculosis* H37Rv sonicates, were inoculated with a 5 mg mixture of polymerized Rv0180c peptides. The mixture included peptides 28624 (CG$^{141}$STNPRAGTLAASIAGQTLTR$^{160}$ GC), 28626 (CG $^{261}$VNISRFRTLLVKWAVMVVLA$^{280}$ GC), 28628 (CG $^{361}$WLAQFEPMHQVFLGVRSLLY$^{380}$ GC). Also, one non-reactive rabbit was inoculated with a polymeric form of peptide 36197 (CG$^{126}$ SAVTPTRTDRPAITISTNPR$^{145}$ GC). Polymers were administered on days 0, 20 and 40 emulsified in Freund's Incomplete Adjuvant (FIA) (Sigma). Bleeding was carried out 20 days after the third inoculation. The Rv0180c peptides used for animal immunizations were chosen by using the BepiPred 1.0b Server epitope prediction software available at http://www.cbs.dtu.dk/services/BepiPred/.

### 2.9. SDS-PAGE and immunoblotting

Sonicates and subcellular fractions of *M. tuberculosis* H37Rv were separated in a discontinuous SDS-PAGE system, transferred to nitrocellulose membrane by the semidry blotting technique and cut into strips [42]. Commercial molecular weight markers (NEB, Inc. Beverly, MA) were used for estimating molecular weights based on migration distances. Strips were incubated with sera obtained from immunized animals diluted 1:100 (v/v) in 5% skimmed milk Tris-Buffered Saline Tween 20 (TBST, containing 0.02 M Tris–HCl, pH 7.5, 0.05 M NaCl) and 1% Tween 20. After five washes with TBST, strips were incubated for 1 h with 1:3000 alkaline phosphatase conjugated anti-goat IgG antibody (ICN Biomedicals, Costa Mesa, CA) and the reaction was developed with NBT/BCIP (KPL, Gaithersburg, MD).

### 2.10. Immunoelectron microscopy (IEM)

Immunoelectron microscopy studies were carried out in a HITACHI HU-12A transmission electronic microscope. Briefly, wet pellet of *M. tuberculosis* H37Rv was fixed using a 4% paraformaldehyde/0.5% glutaraldehyde solution for 2 h at 4 °C. After being fixed, the pellet was dehydrated in graded-ethanol (50–100%) and then embedded in LR-white hard-grade resin (Sigma). Resin polymerization was carried out using a specific cold accelerator [23]. Thin sections of about 400 nm were cut and mounted on 300-mesh nickel grids covered with collodion as support. Grids were then blocked with 5% BSA and 0.1% Tween 20 for 30 min, followed by immersion of the grids in a 1:20 solution of primary antibody at 4 °C overnight. Grids were washed several times with a 0.5% BSA and 0.1% Tween 20 solution and then incubated with 5 nm gold-labeled anti-goat IgG (Sigma) antibody for 1 h at room temperature [72]. Finally, grids were incubated in 6% uranyl acetate for 15 min prior to microscopic examination.

### 2.11. Invasion inhibition assays

Following a previously reported protocol [17] with some modifications, $1 \times 10^6$ A549 and U937 cells suspended in incomplete RPMI 1640 medium were incubated for 1 h in the presence of 50 μM, 100 μM or 200 μM concentrations of HABPs, according to their binding specificity. Subsequently, $1 \times 10^7$ *M. tuberculosis* H37Rv bacilli stained with 20× SYBR Safe (MOI 1:10) were added. These samples were incubated at 37 °C overnight and then enriched with 20 μg/mL of amikacin-supplemented medium (ICN Biomedicals, Costa Mesa, CA). Cells were pelleted by centrifugation at $1000 \times g$ for 5 min, washed twice and fixed in 1% paraformaldehyde (Merck, Darmstadt, Germany), then diluted in RPMI 1640 at 4 °C for 1 h and finally washed and resuspended in RPMI 1640. Cells were counterstained with freshly prepared 3% Methylene Blue (Merck, Germany) for flow cytometry analysis. As negative control, an invasion assays were carried out under the same conditions described above but it was incubated for 2 h with 3 μM Cytochalasin D (SIGMA, St. Louis, MO) as invasion inhibitor. Samples were quantified using a FACScan cytometer (Becton Dickinson), equipped with a 488-nm argon laser. Data were obtained and analyzed using Cellquest software (Becton Dickinson). Uninfected epithelial cells were discriminated from infected epithelial cells according to light FL1 characteristics. A two-tailed student's *t*-test was used to assess differences between treatments.

### 2.12. Internalization of latex beads

Following the procedure described by El-Shazly with some modifications [24]. Briefly, $1 \times 10^6$ A549 cells suspended in incomplete RPMI 1640 medium were grown overnight on a 6-well Multiwell Plate. Fluorescent latex beads ($10 \times 10^6$ beads), beads diameter: 1 μm; (Sigma) were coated with chosen Rv0180c peptides (100 μM), by incubation in incomplete RPMI 1640 medium at 37 °C for 2 h. Peptide-coated beads were then incubated with the cells for 3 h at 37 °C. Cells were washed thrice with Hank's balanced salt solution (HBSS) and dislodged with a 0.6% trypsin (Sigma) and 0.2% EDTA (Sigma) solution. Cells were centrifuged at $1000 \times g$ for 5 min and suspended in 1 mL of incomplete RPMI 1640. Internalization of latex beads was quantified by flow cytometry.

### 2.13. CD spectroscopy

Each HABP was analyzed by CD to evaluate whether there was a correlation between the conformational structures of Rv0180c peptides and their function. CD spectra were acquired at 20 °C on a Jasco J-810 spectropolarimeter at wavelengths ranging from 260 to 190 nm in 1.00-cm cuvettes [54]. Peptides were dissolved to a 0.1 mM concentration in pure water or in 30% (v/v) TFE/water. Each spectrum was obtained by averaging three scans taken at a 20-nm/min scan rate with 1 nm spectra bandwidth and corrected

```
Rv0180c     338  FVILGLPSAGATVPLEAVPAFFRWLAQFEPMHQVFLGVRSLLYL  381  (452)
MAP 3616c   338  FVIFGLPSAGATVPL.ATPPLF.W.AEFEPMHQV..GTRSLLYF  381  (474)
ABC-2       338  FVIFGLPSAGATVPL.ATPPLF.W.AEFEPMHQV..GTRSLLYF  381  (474)
PcMembp     338  FMILGLPSAGATVPL.AVPPFF.W.SEFEPLHQL..GVRSLLYL  381  (465)
cMembp      338  FVILGLPSAGATVPL.AVPPFF.W.AKFEPMHQV..GVRSLLYL  381  (457)
cMembp      338  FVTLGLPSAGATVPL.AVPPFF.W.AKFEPMHQV..GVRSLLYL  381  (457)
HRP-II       23  N.NSAFNNNLCSKNAKGLN.NK.L.HETQAHVDDAHH..HVA..   63  (309)
RIFIN        21  SSYAHNKNKPS.TPHHT.ITTS.V.SEC.LYMPKYDNDADMKSV  64  (343)
Avr1b-1      19  CNATEYSDETNIAMVESPDLVRRSLRNGDIAGGRFLRAHEEDDA  62  (138)
Avr3a        21  LST.NANQAKI.KGTSPGGHSP.L..AYQPDDEGDSPEDRTLSK  64  (111)
```

**Fig. 1.** Alignment of protein fragments from mycobacterial strains, *Plasmodium falciparum* and *Phytophtora sojae* containing the PEXEL motif. From top to bottom: Rv0180c of *M. tuberculosis* H37Rv (CAB09747); hypothetical protein MAP 3616c of *M. avium* subsp. *Paratuberculosis* (AAS06166.1); ABC-2 type transporter family protein of *M. avium* (ABK67761.1); probable conserved membrane protein of *M. leprae* (CAC32132.1); conserved transmembrane protein of *M. marinum* (ACC38890.1); conserved transmembrane protein of *M. ulcerans* (ABL036 66.1); HRP-II of *P. falciparum* (XP_001351080.1); RIFIN of *P. falciparum* (XP_001350951.1); elicitor Avr1b-1 of *P. sojae* (AAR05402.1); avirulence effector protein Avr3a of *P. sojae* (ABQ81647.1). The numbers shown at the beginning and end of the protein fragments indicated the position of such fragment in the protein, while numbers shown in parenthesis indicate the total length of the proteins.

for baseline deviation. The results were expressed as mean residue ellipticity [$\theta$], the units being degrees centimeter squared per decimole of residues, according to the function $[\theta] = \theta_\lambda/(100lcn)$, where $\theta_\lambda$ is the measured ellipticity, $l$ is the optical path length, $c$ is the peptide concentration, and $n$ is the number of amino acid residues in the peptide sequence [65].

## 3. Results

### 3.1. Bioinformatics analysis

The *Rv0180c* gene consists of an open reading frame of 1359 bp and encodes a hypothetical 452-amino-acid-long alanine- and leucine-rich transmembrane protein with a theoretical molecular mass of 47.59 kDa. The protein product has a grand average hydropathicity (GRAVY) index of 0.482 and contains a signal peptide at its N-terminus (signal peptide probability: 0.937) with a cleavage site occurring most likely between positions 41 and 42 (Max cleavage site probability: 0.906). Sequence analysis using the TMHMM Server v. 2.0 showed six transmembrane helices defined as follows: i25–47o; o218–240i; i269–291o; o301–323i; i330–352o and o392–414i, where 'i' refers to inside and 'o' to outside. Protein localization was confirmed by Western blot and IEM, as will be discussed later. A secondary structure prediction obtained by using the SOPMA prediction tool indicated the presence of several α-helical structures. The secondary structure of the HABPs found in Rv0180c was then confirmed by CD spectroscopy.

A BLAST analysis showed 76% and 100% sequence identity of Rv0180c with the probable conserved transmembrane proteins Mb0186c from *Mycobacterium bovis* and ML2600c from *Mycobacterium leprae*, respectively. Among the genus *Mycobacterium*, Rv0180c shares high sequence similarity with transmembrane proteins of *Mycobacterium marinum* (81%), *Mycobacterium ulcerans* (80%), *Mycobacterium kansasii* (82%) and hypothetical proteins of *Mycobacterium avium* subsp. *paratuberculosis* (84%).

Moreover, two possible functional PEXEL-like motifs were identified in Rv0180c. Such motifs comprise amino acids 98–102 (RRLID) and 360–364 (RWLAQ). PEXEL-like motifs were found in proteins from *Mycobacterium* spp., *Plasmodium falciparum* and *Phytophtora sojae* that share high degree of sequence similarity with Rv0180c (Fig. 1).

### 3.2. Identification of the Rv0180c gene in the M. tuberculosis complex

A 346-bp band was amplified by PCR from genomic DNA of species belonging to the *M. tuberculosis* complex (MTBC) using primers specific for *Rv0180c* (Fig. 2A). No amplification was observed in any of the seven strains of mycobacteria other than tuberculosis (MOTT) tested in this study (Fig. 2A). RT-PCR assays were performed only with PCR-positive strains and showed transcription of *Rv0180c* among the MTBC, except in *M. microti* (Fig. 2B). The *rpoB* gene used as positive control for RT-PCR assays was amplified in all tested strains and species from the MTBC, including *M. microti*, which confirms the integrity of the cDNA tested in these assays (Fig. 2C).

### 3.3. Western blotting and immunoelectron microscopy (IEM) studies

Western blot analysis of *M. tuberculosis* H37Rv sonicates with sera raised against polymeric peptides of Rv0180c (post-third immunization sera) recognized two bands of about 48 and 63 kDa (Fig. 3A, lane 2), whereas pre-immune sera from the same animals showed no reactivity to any mycobacterial protein. The ~48 kDa band is close to the theoretical molecular mass of Rv0180c (47.59 kDa), while the second band is probably the result micro-

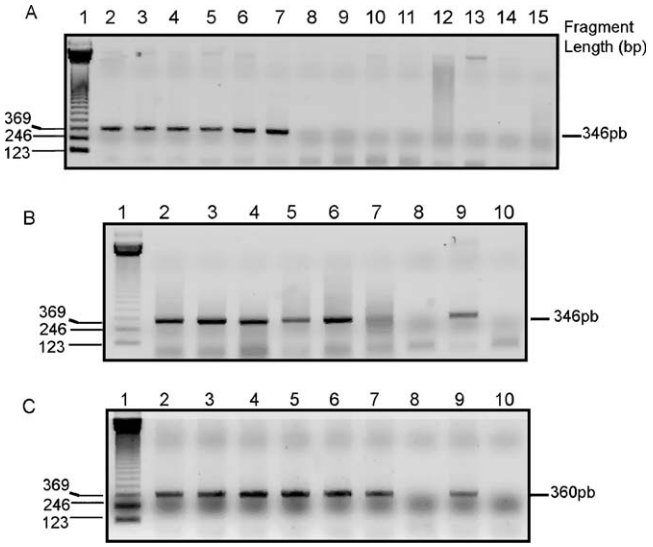


**Fig. 2.** Assessment of the presence and transcription of the *Rv0180c* gene in the MTBC and MOTT. (A) A 346-bp PCR product corresponding to the *Rv0180c* gene was amplified from genomic DNA of strains and species belonging to the MTBC but no amplification product was observed in MOTT. (1) 1-kb DNA ladder; (2) *M. tuberculosis* H37Rv; (3) *M. tuberculosis* H37Ra; (4) *M. bovis*; (5) *M. bovis*-BCG; (6) *M. africanum*; (7) *M. microti*; (8) *M. flavescens*; (9) *M. fortuitum*; (10) *M. szulgai*; (11) *M. peregrinum*; (12) *M. phlei*; (13) *M. scrofulaceum*; (14) *M. avium*; (15) PCR negative control. (B) Amplification of a 346-bp RT-PCR amplicon corresponding to the *Rv0180c* gene from cDNA of MTBC strains. (1) 1-kb DNA ladder; (2) *M. tuberculosis* H37Rv; (3) *M. tuberculosis* H37Ra; (4) *M. bovis*; (5) *M. bovis*-BCG; (6) *M. africanum*; (7) *M. microti*; (8) Negative control (*M. tuberculosis* DNA treated with DNAse I); (9) PCR positive control (*M. tuberculosis* H37Rv DNA); (10) PCR negative control. (C) RT-PCR amplification of the *rpo*B gene corresponding to the RNA polymerase (β-subunit) as positive transcription control in the same strains (360-bp fragment).

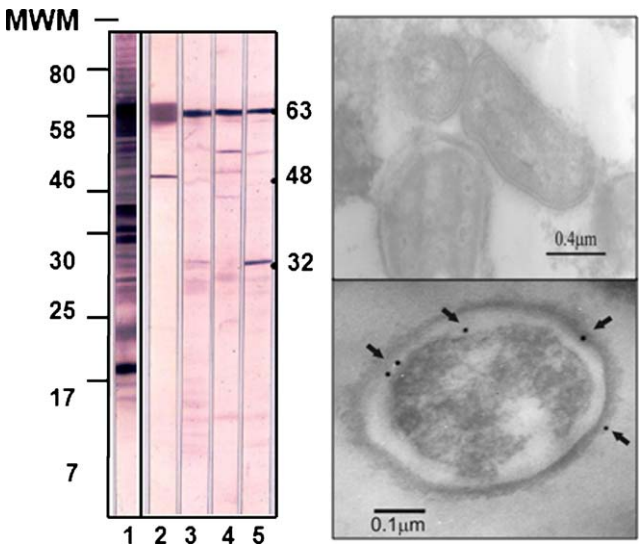


**Fig. 3.** Expression and subcellular localization of Rv0180c. (A) Western blot analyses with sera post-3rd immunization raised against polymeric peptides of Rv0180c. Lane 1: hyperimmune sera raised against the whole *M. tuberculosis* sonicate; lane 2: sera obtained against peptides of Rv0180c versus *M. tuberculosis* sonicate; lane 3: cell membrane; lane 4: cell wall; lane 5: cytosol fraction. MWM: molecular weight marker. (B) Top panel: control IEM assay with preimmune serum showing no immunolabeling (amplification: 5000×). Bottom panel: localization of the Rv0180c protein in the envelope of *M. tuberculosis* H37Rv bacilli. Gold-labeled particles observed on mycobacterial surface are indicated by black arrows (amplification: 5000×).

heterogeneity caused by posttranslational modifications such as the oxidation of side chains, as it has been previously reported for other mycobacterial proteins [75], and is consistent with sequence analyses showing that Rv0180c has several probable glycosylation sites (Fig. 4).

Other results were obtained in immunoblotting assays with subcellular fractions of *M. tuberculosis* H37Rv (Fig. 3A), where the 48-kDa band was detected only in cell wall (lane 4), while the 63-kDa band was detected in cellular membrane (lane 3), cell wall (lane 4) and cytosol (lanes 5). An additional band on 32kDa was found in cytosol suggesting a proteolytic process (lane 5). Protein recognition by serum raised against *M. tuberculosis* H37Rv sonicate (lane 1) and the molecular weight patterns are also shown in Fig. 3A.

IEM studies with serum raised against peptide 36197 showed colloidal gold particles (10 nm) on the surface of *M. tuberculosis* H37Rv bacilli (Fig. 3B, lower photograph), while no particles were observed when the assay was carried out with pre-immune serum (Fig. 3B, upper photograph). These results agree with the predicted transmembrane localization of Rv0180c.

### 3.4. High activity binding peptides

Binding assays with $^{125}$I-radiolabeled peptides have been shown to be an effective way to identify and characterize peptides of mycobacterial proteins binding specifically and with high activity to U937 and A549 cells, considering that these two cells lines are excellent *in vitro* models for the study of *M. tuberculosis* invasion [21,26,29]. Specific binding activity is defined as the slope of the curve obtained by plotting the amount of specifically bound $^{125}$I-labeled peptide per added $^{125}$I-labeled peptide, where pep-

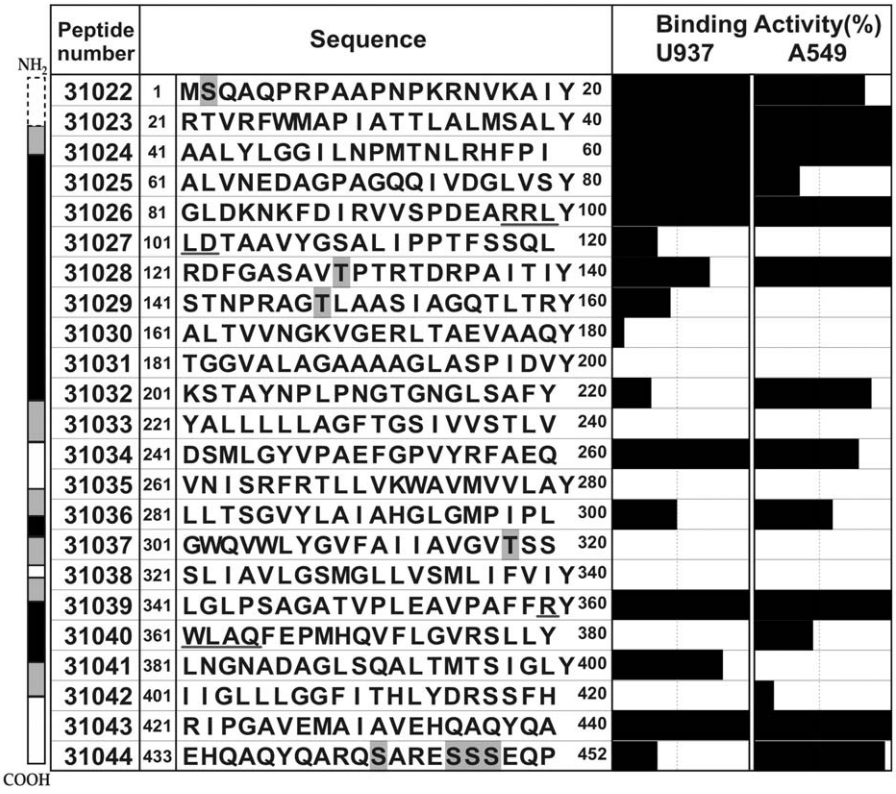


**Fig. 4.** Topology and cell binding profile of the Rv0180c protein. The topology shown on the left indicates the position of different protein domains and motifs: transmembrane domains (unfilled bars), outer protein domains (filled bars), signal peptide (SP), and transmembrane helices predicted by the TMHMM server (gray bars). The right-hand chart shows the specific cell binding activity of each of the Rv0180c peptides, which were named according to our institute's serial numbering system. The specific binding activity to A549 and U937 cells is represented by the horizontal black bars shown to the right of each peptide sequence. Numbers shown at beginning and end of the sequences indicate the position of the peptide in the native protein. Peptides with slope of ≥1% were considered to be HABP. Nd: no data available due to solubility problems. Underlined residues correspond to the HTC signals or PEXEL motifs predicted by the Scanprosite server. Possible glycosylation sites are highlighted in gray.

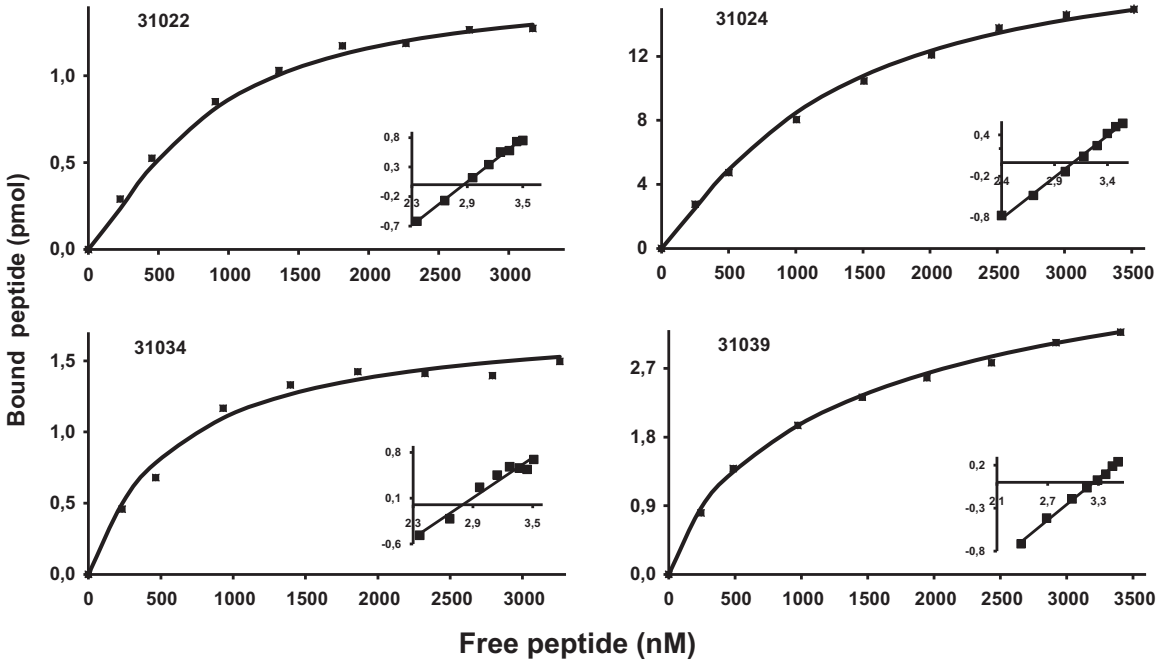


**Fig. 5.** Saturation assays. Saturation curves obtained for HABPs 31022, 31024, 31034 and 31039, all of which bind to the U937 cell line. Saturation curves were obtained by plotting the amount of specifically bound $^{125}$I-HABP versus the amount of free $^{125}$I-HABP. Inset: Hill plot, where the abscissa is $\log F$ and the ordinate is $\log[B/B_m - B]$, $B_m$ being the maximum amount of bound peptide, $B$ the amount of bound peptide and $F$ the amount of free peptide.

tides showing a specific binding activity equal to or higher than 1% are considered HABPs [26,53]. Fig. 4 shows the sequences of the 23 peptides resulting from dissecting the amino acid sequence of Rv0180c into 20-mer-long non-overlapping peptides, with their corresponding binding activities to U937 and A549 cells. A total of 13 HABPs were found in Rv0180c, of which peptides 31022, 31023, 31024, 31026, 31028, 31034, 31036, 31039 and 31043 showed specific binding activity to both cell lines, whereas peptides 31032 and 31044 bound exclusively to A549 cells and peptides 31025 and 31041 bound exclusively to the U937 cell line.

### 3.5. Saturation assays

Based on the results of binding assays, HABPs 31022, 31024, 31034 and 31039 were selected in order to characterize binding interactions between Rv0180c HABPs and U937 cells (Fig. 5). Saturation curve and Hill analysis were performed and dissociation constants ($K_d$) of 800, 1000, 600 and 1700 nM were obtained for each of these HABPs, respectively. Hill coefficients ($n_H$) of 1.34, 1.2 and 1.02 were obtained for HABPs 31022, 31024 and 31034, respectively, which suggest positive cooperativity for these ligand–receptor interaction, whereas HABP 31039 showed negative ligand–receptor cooperativity ($n_H = 0.8$). Regarding to the number of receptor for these HABPs on U937 cells, $7.5 \times 10^5$, $1.6 \times 10^5$, $9.0 \times 10^5$ and $2.5 \times 10^6$ binding sites per cell were calculated for these HABPs, respectively.

### 3.6. Invasion inhibition assay using HABPs

Invasion inhibition assays were carried out with HABPs 31022–31026, 31028, 31032, 31034, 31036, 31039, 31041 and 31043 in order to evaluate the effect of HABPs on mycobacterial invasion of either A549 or U937 cells. Peptides 31027 and 31032 were used as negative controls for invasion inhibition assays in A549 and U937 cells, respectively. In general, HABPs 31023, 31024 and 31026 inhibited invasion of A549 and U937 cells, while no decrease in the invasion to either cell line was observed in assays with HABP 31022, probably due to its possible role as signal peptide (Fig. 6). HABPs 31023, 31024, 31025, 31026, 31036, 31039, 31041 and 31043 inhibited of invasion of U937 cells at all tested concentrations (Fig. 6, upper), however only HABPs 31025 and 31026 showed a concentration-dependent inhibition behavior. Likewise, HABPs 31023, 31024, 31026, 31028, 31032, 31034 and 31039 were able to decrease significantly invasion of A549 cells by *M. tuberculosis* (Fig. 6, lower).

### 3.7. Internalization of HABP-coated latex beads by HeLa cells

Previous studies have shown the utility of using fluorescent protein-coated latex beads to study uptake and internalization of *M. tuberculosis* proteins by non-phagocytic cells (HeLa cells) [19,24], hence, in this study we wanted to determine if latex beads coated with purified synthetic peptides of Rv0180c were internalized by A549 cells. A total of fifteen peptides of Rv0180c were analyzed in internalization assays, finding a maximum internalization peak of $20.24 \pm 2.25\%$ for HABP 31024 and a minimum internalization percentage of $0.9 \pm 0.2\%$ for peptide 31031 (Fig. 7). A modified internalization assay (control treatment) that consisted in incubating cells with the peptide directly with the cells and then adding latex beads was carried out, in order to differentiate the peptide's effect on these cells, i.e., to determine if latex bead internalization was induced by the peptide coating the latex beads or by the peptide alone. As it can be observed in Fig. 7, HABPs 31022–31024, 31026, 31034, 31036 and 31043 caused significant internalization of latex beads, whereas the internalization percentage of the control treatment was always lower than the percentages obtained with peptide-coated beads. Not all HABPs induced significant internalization of latex beads, which suggests that only some HABPs of Rv0180c may have important roles during cell invasion.

### 3.8. Circular dichroism spectroscopy

Circular dichroism (CD) spectroscopy was used to obtain information about the secondary structure for all the non-overlapping

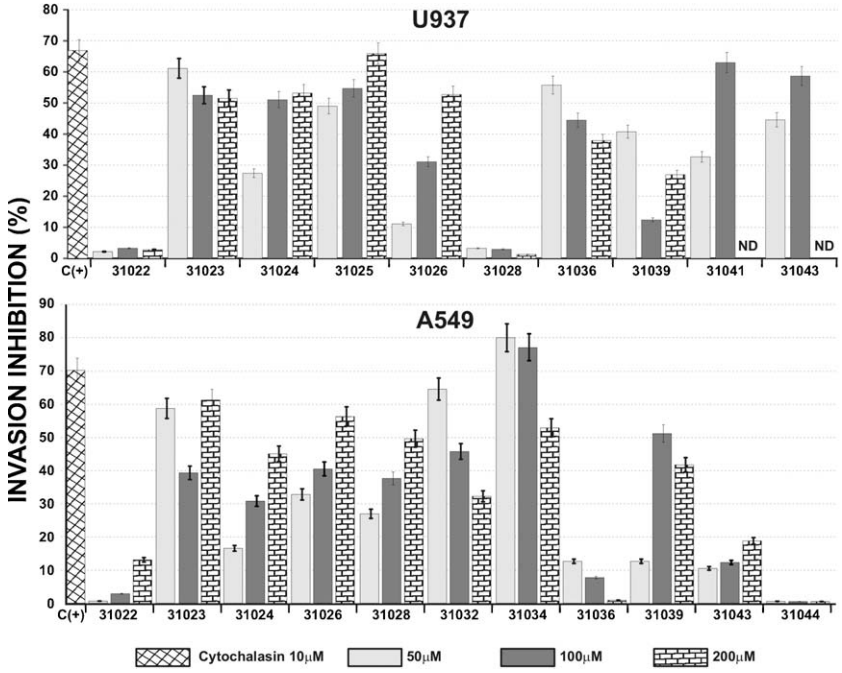


**Fig. 6.** Invasion inhibition assays. (A) Percentage of mycobacterial invasion to U937 cells with different concentrations of Rv0180c HABPs. (B) Percentage of mycobacterial invasion to A549 cells with different concentrations of Rv0180c HABPs. Cytochalasin D (actin polymerization inhibitor) is used as positive control of invasion inhibition (crisscross grid). The results correspond to the average percentage of invasion calculated for each treatment ± standard deviation. $^{*}p \leq 0.05$; $^{**}p \leq 0.01$, according to a two tailed student's *t*-test.

peptides of Rv0180c. In general, Rv0180c peptides displayed different CD profiles in water (data not shown), which corresponded to their typical structural organizations that were further stabilized in 30% TFE solution. Fig. 8A shows the CD profiles of all the peptides displaying spectra typical of α-helical structures. These results are in agreement with the secondary structure predicted for Rv0180c by the self-optimized prediction method with alignment (SOPMA), however SOPMA predicted more α-helices that those identified by CD (Fig. 8B). No β-sheet profiles were identified in the CD spectra of any of the peptides. SOPMA is a useful tool for predicting the secondary structures of proteins, but its predictions should be confirmed and supported by a robust methodology such as CD spectroscopy, as performed in this study.

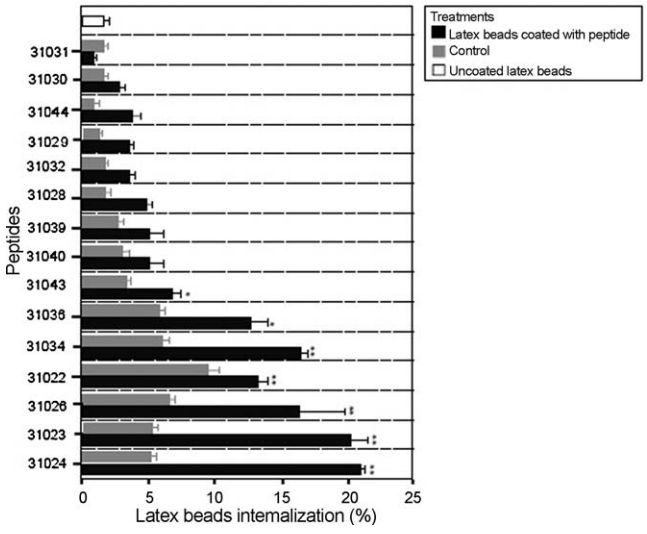


**Fig. 7.** Percentages of peptide-coated latex beads internalized by A549 cells. A549 cells were independently incubated with peptides and then with uncoated latex beads as control treatment. The results correspond to average internalization calculated for each treatment ± SD. $^{*}p \leq 0.01$; $^{**}p \leq 0.001$, according to a two tailed student's *t*-test.

## 4. Discussion

TB continues to be one of the major causes of disease worldwide despite the existence of effective drug treatments and vaccination with the Calmette-Guérin (BCG) bacilli, which has been given to more people than any other vaccine in the history of human kind [40]. Vaccination with BCG has varying protective efficacy against pulmonary TB in adults, which together with the high cost and log-term administration of anti-TB drug treatments, made it necessary to develop new and improved prophylactic and therapeutic strategies to control the spread of this disease.

Some of the most efficient anti-TB treatments are targeted to mycobacterial wall and protein synthesis. Many studies have screened the *M. tuberculosis* H37Rv proteome in the search for candidate molecules to design novel prevention strategies and treatment options for TB. Despite all efforts, little is known about the role played by *M. tuberculosis* proteins in host-cell invasion and survival of bacilli inside macrophages and epithelial monocytes. Surface proteins act both as interface and barriers between the bacteria and the host cell, thus they have become subjects of intense research [15]. Bearing this in mind, our group has determined the presence, transcription and expression of five *M. tuberculosis* membrane proteins: Rv2004c, Rv2536, Rv1510c, Rv2560, Rv2707, Rv1980c and Rv0679c [12,18,26,29,53,58,70]. In addition, the binding profiles of each of these proteins to A549 and U937 cell lines has been determined by means of binding assays with non-overlapping synthetic peptides spanning the entire length of each protein. Such studies constitute an initial step in the rational selection of components for a subunit-based chemically synthesized anti-TB vaccine and are waiting for future trials in animal models.

This study focused on Rv0180c, which is an alanine- and leucine-rich protein that is hypothesized to be a transmembrane protein because of its hydrophobic character (GRAVY score: 0.48), the pres-

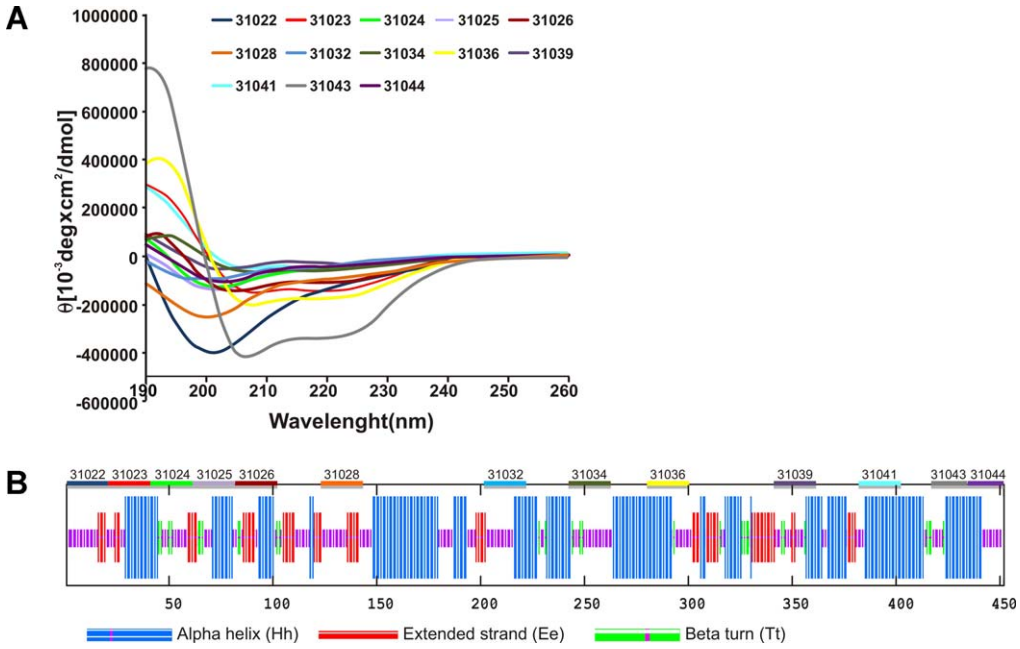


**Fig. 8.** CD spectra and secondary structure SOPMA prediction for Rv0180c. (A) The spectra of HABPs displayed characteristic α-helical profiles that agree with the α-helical conformation predicted by SOPMA. (B) Secondary structure prediction by SOPMA. Upper horizontal bars indicate the localization of each of the Rv0180c peptides for which CD spectra are shown in (A).

ence of six predicted transmembrane helices and homology to the probable conserved transmembrane proteins ML2600c from *M. leprae* and Mb0186c from *M. bovis*. In this study the localization of Rv0180c in the surface of *M. tuberculosis* was confirmed by IEM.

Sequence analysis using bioinformatics tools shows the presence of a PEXEL-like motif, which has not been previously reported in mycobacterial proteins. In general, the PEXEL motif has been shown to have a targeting and signaling function in other intracellular parasites such as *P. falciparum* and *P. infestans*. In *P. falciparum* the PEXEL motif has been involved in the delivery, export and trafficking of parasite proteins to the host cells [35,46,77], which makes it plausible to suppose a similar function for this motif in the mycobacterial protein Rv0180c. The presence of this motif was also found here in Rv0180c homologues from five other virulent strains of mycobacteria; however, the possible role of this motif during mycobacterial invasion or survival inside target cells has not been studied up to date. Consequently, the presence, transcription and expression of the *Rv0180c* gene in virulent and avirulent mycobacterial strains were assessed by PCR amplification. The *Rv0180c* gene was identified in species and strains belonging to the MTBC, except for *M. microti*. Gene transcription was detected in the same MTBC strains. The recognition of Rv0180c by the sera raised against peptides derived from Rv0180c in Western blot analysis of *M. tuberculosis* H37Rv sonicates confirms the expression of the encoded protein in *M. tuberculosis* H37Rv. The same sera confirmed the presence of Rv0180c in the surface of *M. tuberculosis* H37Rv bacilli by IEM, thus showing that both the native and denatured forms of the protein were being recognized.

A noteworthy number of 13 HABPs out of the total 23 peptides comprising the sequence of Rv0180c were identified in binding assays with A549 and U937 cells. Nine of the 13 HABPs were specific for both cell lines, two for A549 cells and two for U937 cells. Saturation assays with HABPs showed a strong binding cooperativity, as shown by the dissociation constants and Hill coefficients of four of these HABPs.

There are several well known receptors for *M. tuberculosis* in macrophages, such as complement receptors (Crs), Mannose receptors (Mrs), Surfactant protein A receptors (SP-A receptors), and CD14 among others, that could be interacting and affecting the macrophage response to invasion by this pathogen [11,25]. Additional studies would allow testing the role and importance of the interaction between the Rv0180c HABPs herein identified and different host-cell surface receptors. Moreover, internalization assays with latex beads coated with Rv0180c HABPs suggest that these peptides could be mediating uptake and internalization of latex beads by A549 cells, thus supporting a possible role of Rv0180c HABPs in the invasion of mammalian cells.

In addition to the possible role of Rv0180c in adapting the host macrophage to the needs of the invading *M. tuberculosis* bacilli, protein regions having high binding activity to host-cell receptors were also able to significantly inhibit invasion of human macrophages by *M. tuberculosis* H37Rv, therefore supporting a possible key role of these protein regions in macrophage invasion and targeting of Rv0180c to the surface of *M. tuberculosis* bacilli. According to CD spectroscopy studies and SOPMA predictions, the secondary structure of the protein contains seven α-helical peptides, which further supports the transmembrane localization of Rv0180c.

With the aim of blocking completely the mycobacterium entry to target cells, taking into account the variety of entrance alternatives that this microorganism present, our proposal is based on the identification of protein fragments, which interact with host cells. The proteins of departure will be those that are potentially used by mycobacteria due to its localization characteristics [63], or proposed in previous articles or bioinformatics analyses [57,71], to establish an initial contact with the host cell.

It has been reported that a considerable number of secreted proteins are protective antigens, and therefore have been considered as attractive candidates to develop subunit vaccines [3,33,36], or proteins that bind to the host cell and that can be used in designing diagnostic methods [62] Moreover, they are hypothesized to mediate mycobacterial entry into the host cell [59].

The methodology used here for identifying binding fragments from the selected proteins has been previously applied in *P. falciparum* studies [4,28,30,31,44,55,68,69], *Plasmodium vivax* [48,67] and *M. tuberculosis* [12,18,26,49,50,53,58,70]. In the case of *P. falciparum*, identified sequences have been the base to the ratio-

nal design of subunit-based, multiantigenic, multistage chemically synthesized vaccines, and a universal methodology has been proposed, that might be applied to prevent different infectious diseases [13,51,52]. For *M. tuberculosis* proteins, and specifically for Rv0180c, identified HABPs capable of inhibiting mycobacterial entry to host cells could be included in immunological studies using animal models, to assess their potential as components of a subunit-based anti-tuberculous vaccine.

The use of HABPs-based sequences in tuberculosis is supported on the fact that the immune response against extracellular microorganisms has been proposed to be mainly mediated by antibodies, while the cellular immune response is directed against intracellular microorganisms. However, it is not clear if, *in vivo*, there is a total independence between the immune response mediated by antibodies and the immune response mediated by cells [39,45]; therefore, taking into account the variety of broad interactions of B lymphocytes with cellular immunity, B cells might have a significant impact on the outcome of airborne challenge with *M. tuberculosis*, as well as in the resultant inflammatory response.

## Acknowledgements

The materials used in this study were received as part of the NIH, NIAID Contract No. HHSN266200400091C, entitled "Tuberculosis Vaccine Testing and Research Materials," which was awarded to the Colorado State University. *M. tuberculosis* subcellular protein fractions were obtained through the National Institute of Health (NIH), National Institute of Allergy and Infectious Diseases (NIAID) contract HHSN266200400091C, "Tuberculosis Vaccine Testing and Research Materials," awarded to Dr. J. Belisle, Colorado State University (Fort Collins, CO, USA). Also, we would like to thank Nora Martinez for translating and revising the manuscript.

## References

[1] Altschul SF, Madden TL, Schaffer AA, Zhang J, Zhang Z, Miller W, et al. Gapped BLAST and PSI-BLAST: a new generation of protein database search programs. Nucleic Acids Res 1997:3389–402.
[2] Allen R, Bittner-Eddy PD, Grenville-Briggs LJ, Meitz JC, Rehmany AP, Rose LE, et al. Host–parasite co-evolutionary conflict between Arabidopsis and downy mildew. Science 2004:1957–60.
[3] Andersen P, Askgaard D, Ljungqvist L, Bentzon MW, Heron I. T-cell proliferative response to antigens secreted by *Mycobacterium tuberculosis*. Infect Immun 1991;59:1558–63.
[4] Arevalo-Pinzon G, Curtidor H, Vanegas M, Vizcaino C, Patarroyo MA, Patarroyo ME. Conserved high activity binding peptides from the *Plasmodium falciparum* rhoptry protein inhibit merozoites in vitro invasion of red blood cells Peptides 2010, doi:10.1016/j.peptides.2010.07.009, in press.
[5] Armstrong MR, Whisson SC, Pritchard L, Bos JI, Venter E, Avrova AO, et al. An ancestral oomycete locus contains late blight avirulence gene Avr3a, encoding a protein that is recognized in the host cytoplasm. Proc Natl Acad Sci U S A 2005;102:7766–71.
[6] Beatty WL, Rhoades ER, Ullrich HJ, Chatterjee D, Heuser JE, Russell DG. Trafficking and release of mycobacterial lipids from infected macrophages. Traffic 2000:235–47.
[7] Beatty WL, Russell DG. Identification of mycobacterial surface proteins released into subcellular compartments of infected macrophages. Infect Immun 2000;68:6997–7002.
[8] Bendtsen JD, Nielsen H, Von Heijne G, Brunak S. Improved prediction of signal peptides: SignalP 3.0. J Mol Biol 2004;340:783–95.
[9] Birch PRJ, Rehmany AP, Pritchard L, Kamoun S, Beynon JL. Trafficking arms: oomycete effectors enter host plant cells. Trends Microbiol 2006;14:8–11.
[10] Bos JIB, Kanneganti TD, Young C, Cakir C, Huitema E, Win J, et al. The C-terminal half of *Phytophthora infestans* RXLR effector AVR3a is sufficient to trigger R3a-mediated hypersensitivity and suppress INF1-induced cell death in *Nicotiana benthamiana*. Plant J 2006;48:165–76.
[11] Bowdish DM, Sakamoto K, Kim MJ, Kroos M, Mukhopadhyay S, Leifer CA, et al. MARCO, TLR2, and CD14 are required for macrophage cytokine responses to mycobacterial trehalose dimycolate and *Mycobacterium tuberculosis*. PLoS Pathogens 2009;5:e1000474.
[12] Cifuentes DP, Ocampo M, Curtidor H, Vanegas M, Forero M, Patarroyo ME, et al. *Mycobacterium tuberculosis* Rv0679c protein sequences involved in host-cell infection: potential TB vaccine candidate antigen. BMC Microbiol 2010;10:109.
[13] Cifuentes G, Bermudez A, Rodriguez R, Patarroyo MA, Patarroyo ME. Shifting the polarity of some critical residues in malarial peptides' binding to host cells is a key factor in breaking conserved antigens' code of silence. Med Chem 2008;4:278–92.
[14] Cole ST, Brosch R, Parkhill J, Garnier T, Churcher C, Harris D, et al. Deciphering the biology of *Mycobacterium tuberculosis* form the complete genome sequence. Nature 1998;393:537–44.
[15] Colston MJ. The molecular basis of mycobacterial infection. Mol Aspects Med 1996;17:383–454.
[16] Chang ST, Linderman JJ, Kirschner DE. Multiple mechanisms allow *Mycobacterium tuberculosis* to continuously inhibit MHC class II-mediated antigen presentation by macrophages. Proc Natl Acad Sci U S A 2005;102:4530–5.
[17] Chapeton-Montes JA, Plaza DF, Barrero CA, Patarroyo MA. Quantitative flow cytometric monitoring of invasion of epithelial cells by *Mycobacterium tuberculosis*. Front Biosci 2008;13:650–6.
[18] Chapeton-Montes JA, Plaza DF, Curtidor H, Forero M, Vanegas M, Patarroyo ME, et al. Characterizing the *Mycobacterium tuberculosis* Rv2707 protein and determining its sequences which specifically bind to two human cell lines. Protein Sci 2008;17:342–51.
[19] Chitale S, Ehrt S, Kawamura I, Fujimura T, Shimono N, Anand N, et al. Recombinant *Mycobacterium tuberculosis* protein associated with mammalian cell entry. Cell Microbiol 2001;3:247–54.
[20] Daffe M, Etienne G. The capsule of *Mycobacterium tuberculosis* and its implications for pathogenicity. Tuber Lung Dis 1999;79:153–69.
[21] Danelishvili L, McGarvey J, Li YJ, Bermudez LE. *Mycobacterium tuberculosis* infection causes different levels of apoptosis and necrosis in human macrophages and alveolar epithelial cells. Cell Microbiol 2003;5:649–60.
[22] De Castro E, Sigrist CJA, Gattiker A, Bulliard V, Langendijk-Genevaux PS, Gasteiger E, et al. ScanProsite: detection of PROSITE signature matches and ProRule-associated functional and structural residues in proteins. Nucleic Acids Res 2006:34.
[23] De Souza W. Técnicas de Microscopia Eletrônica Aplicadas às Ciências Biológicas. Sociedade Brasileira de Microscopia 2007:145–63.
[24] El-Shazly S, Ahmad S, Mustafa AS, Al-Attiyah R, Krajci D. Internalization by HeLa cells of latex beads coated with mammalian cell entry (Mce) proteins encoded by the mce3 operon of *Mycobacterium tuberculosis*. J Med Microbiol 2007;56:1145–51.
[25] Ernst JD. Macrophage receptors for *Mycobacterium tuberculosis*. Infect Immun 1998;66:1277–81.
[26] Forero M, Puentes A, Cortes J, Castillo F, Vera R, Rodriguez LE, et al. Identifying putative *Mycobacterium tuberculosis* Rv2004c protein sequences that bind specifically to U937 macrophages and A549 epithelial cells. Protein Sci 2005;14:2767–80.
[27] Frehel C, Chastellier C, Lang T, Rastogi N. Evidence for inhibition of fusion of lysosomal and prelysosomal compartments with phagosomes in macrophages infected with pathogenic *Mycobacterium avium*. Infect Immun 1986;52:252–562.
[28] Garcia J, Curtidor H, Vanegas M, Gabriela AP, Patarroyo MA, Patarroyo ME. Conserved regions of the *Plasmodium falciparum* rhoptry-associated protein 3 mediate specific host-pathogen interactions during invasion of red blood cells. Peptides 2010, doi:10.1016/j.peptides.2010.09.002, in press.
[29] Garcia J, Puentes A, Rodriguez L, Ocampo M, Curtidor H, Vera R, et al. *Mycobacterium tuberculosis* Rv2536 protein implicated in specific binding to human cell lines. Protein Sci 2005;14:2236–45.
[30] Garcia JE, Puentes A, Curtidor H, Vera R, Rodriguez L, Valbuena J, et al. Peptides from the *Plasmodium falciparum* STEVOR putative protein bind with high affinity to normal human red blood cells. Peptides 2005;26:1133–43.
[31] Garcia JE, Puentes A, Lopez R, Vera R, Suarez J, Rodriguez L, et al. Peptides of the liver stage antigen-1 (LSA-1) of *Plasmodium falciparum* bind to human hepatocytes. Peptides 2003;24:647–57.
[32] Geourjon C, Deleage G. SOPMA: significant improvements in protein secondary structure prediction by consensus prediction from multiple alignments. Comput Appl Biosci 1995;11:681–4.
[33] Guerrero GG, Debrie AS, Locht C. Boosting with mycobacterial heparin-binding haemagglutinin enhances protection of *Mycobacterium bovis* BCG-vaccinated newborn mice against *M. tuberculosis*. Vaccine 2010;28:4340–7.
[34] Hiller NL, Bhattacharjee S, Van Ooij C, Liolios K, Harrison T, Lopez-Estraño C, et al. Host-targeting signal in virulence proteins reveals a secretome in malarial infection. Science 2004;306:1934–7.
[35] Hiss J, Przyborski J, Schwarte F, Lingelbach K, Schneider G. The plasmodium export element revisited. PLoS ONE 2008;3:e1560.
[36] Horwitz MA, Lee BW, Dillon BJ, Harth G. Protective immunity against tuberculosis induced by vaccination with major extracellular proteins of *Mycobacterium tuberculosis*. Proc Natl Acad Sci U S A 1995;92:1530–4.
[37] Houghten RA. General method for the rapid solid-phase synthesis of large numbers of peptides: specificity of antigen-antibody interaction at the level of individual amino acids. Proc Natl Acad Sci U S A 1985:82.
[38] Hulme EC. Receptor–ligand interactions. A practical approach. Oxford: IRL Press; 1993.
[39] Igietseme JU, Eko FO, He Q, Black CM. Antibody regulation of T cell immunity: implications for vaccine strategies against intracellular pathogens. Expert Rev Vaccines 2004;3:23–34.
[40] Kaufmann SH. Is the development of a new tuberculosis vaccine possible? Nat Med 2000;6:955–60.
[41] Krogh A, Larsson B, Von Heijne G, Sonnhammer ELL. Predicting transmembrane protein topology with a hidden Markov model: application to complete genomes. J Mol Biol 2001;305:567–80.

[42] Kyhse-Andersen J. Electroblotting of multiple gels: a simple apparatus without buffer tank for rapid transfer of proteins from polyacrylamide to nitrocellulose. J Biochem Biophys Methods 1984;10:203–9.
[43] Kyte J, Doolittle RF. A simple method for displaying the hydropathic character of a protein. J Mol Biol 1982;157:105–32.
[44] Lopez R, Valbuena J, Rodriguez LE, Ocampo M, Vera R, Curtidor H, et al. *Plasmodium falciparum* merozoite surface protein 6 (MSP-6) derived peptides bind erythrocytes and partially inhibit parasite invasion. Peptides 2006;27:1685–92.
[45] Maglione PJ, Chan J. How B cells shape the immune response against *Mycobacterium tuberculosis*. Eur J Immunol 2009;39:676–86.
[46] Marti M, Baum J, Rug M, Tilley L, Cowman AF. Signal-mediated export of proteins from the malaria parasite to the host erythrocyte. J Cell Biology 2005;171:587–92.
[47] Marti M, Good RT, Rug M, Knuepfer E, Cowman AF. Targeting malaria virulence and remodeling proteins to the host erythrocyte. Science 2004;306:1930–3.
[48] Ocampo M, Vera R, Eduardo Rodriguez L, Curtidor H, Urquiza M, Suarez J, et al. Plasmodium vivax Duffy binding protein peptides specifically bind to reticulocytes. Peptides 2002;23:13–22.
[49] Patarroyo MA, Curtidor H, Plaza DF, Ocampo M, Reyes C, Saboya R, et al. Peptides derived from *Mycobacterium tuberculosis* Rv1490 surface protein implicated in inhibition of epithelial cell entry: potential vaccine candidates? Vaccine 2008;26:4387–95.
[50] Patarroyo MA, Plaza DF, Ocampo M, Curtidor H, Forero M, Rodriguez LE, et al. Functional characterization of *Mycobacterium tuberculosis* Rv2969c membrane protein. Biochem Biophys Res Commun 2008;372:935–40.
[51] Patarroyo ME, Cifuentes G, Bermudez A, Patarroyo MA. Strategies for developing multi-epitope, subunit-based, chemically synthesized anti-malarial vaccines. J Cell Mol Med 2008;12:1915–35.
[52] Patarroyo ME, Patarroyo MA. Emerging rules for subunit-based, multiantigenic, multistage chemically synthesized vaccines. Acc Chem Res 2008;41:377–86.
[53] Plaza DF, Curtidor H, Patarroyo MA, Chapeton-Montes JA, Reyes C, Barreto J, et al. The *Mycobacterium tuberculosis* membrane protein Rv2560-biochemical and functional studies. FEBS J 2007;274:6352–64.
[54] Provencher SW, Glockner J. Estimation of globular protein secondary structure from circular dichroism. Biochemistry 1981;20:33–7.
[55] Puentes A, Garcia J, Ocampo M, Rodriguez L, Vera R, Curtidor H, et al. *P. falciparum*: merozoite surface protein-8 peptides bind specifically to human erythrocytes. Peptides 2003;24:1015–23.
[56] Rehmany A, Gordon A, Rose LE, Allen RL, Armstrong MR, Whisson SC, et al. Differential recognition of highly divergent downy mildew avirulence gene alleles by RPP1 resistance genes from two Arabidopsis lines. Plant Cell 2005;17:1839–50.
[57] Restrepo-Montoya D, Vizcaino C, Nino LF, Ocampo M, Patarroyo ME, Patarroyo MA. Validating subcellular localization prediction tools with mycobacterial proteins. BMC Bioinformatics 2009;10:134.
[58] Rodriguez D, Vizcaino C, Ocampo M, Curtidor H, Pinto M, Patarroyo ME, et al. Peptides from the *Mycobacterium tuberculosis* Rv1980c protein involved in human cell infection: insights into new synthetic subunit vaccine candidates. Biol Chem 2010;391:207–17.
[59] Saini NK, Sharma M, Chandolia A, Pasricha R, Brahmachari V, Bose M. Characterization of Mce4A protein of *Mycobacterium tuberculosis*: role in invasion and survival. BMC Microbiol 2008;8:200.
[60] Sargeant TJ, Marti M, Caler E, Carlton JM, Simpson K, Speed TP, et al. Lineage-specific expansion of proteins exported to erythrocytes in malaria parasites. Genome Biol 2006;7:R12.
[61] Shan W, Cao M, Leung D, Tyler BM. The Avr1b locus of *Phytophthora sojae* encodes an elicitor and a regulator required for avirulence on soybean plants carrying resistance gene *Rps1b*. Mol Plant Microbe Interact 2004;17:394–403.
[62] Shin AR, Lee KS, Lee JS, Kim SY, Song CH, Jung SB, et al. *Mycobacterium tuberculosis* HBHA protein reacts strongly with the serum immunoglobulin M of tuberculosis patients. Clin Vaccine Immunol 2006;13:869–75.
[63] Song H, Sandie R, Wang Y, Andrade-Navarro MA, Niederweis M. Identification of outer membrane proteins of *Mycobacterium tuberculosis*. Tuberculosis (Edinb) 2008;88:526–44.
[64] Sonnhammer ELL, Von Heijne G, Krogh A. A hidden Markov model for predicting transmembrane helices in protein sequences. In: Glasgow J, Littlejohn T, Major F, Lathrop R, Sankoff D, Sensen C, editors. Sixth international conference on intelligent systems for molecular biology. Menlo Park, CA: AAAI Press; 1998. p. 175–82.
[65] Sreerama N, Venyaminov SY, Woody RW. Estimation of the number of a-helical and b-strand segments in proteins using circular dichroism spectroscopy. Protein Sci 1999;8:370–80.
[66] Sterne JAC, Rodrigues LC, Guedes IN. Does the efficacy of BCG decline with time since vaccination? Int J Tuberc Lung Dis 1998;2:200–7.
[67] Urquiza M, Patarroyo MA, Mari V, Ocampo M, Suarez J, Lopez R, et al. Identification and polymorphism of *Plasmodium vivax* RBP-1 peptides which bind specifically to reticulocytes. Peptides 2002;23:2265–77.
[68] Urquiza M, Rodriguez LE, Suarez JE, Guzman F, Ocampo M, Curtidor H, et al. Identification of *Plasmodium falciparum* MSP-1 peptides able to bind to human red blood cells. Parasite Immunol 1996;18:515–26.
[69] Valbuena JJ, Vera R, Garcia J, Puentes A, Curtidor H, Ocampo M, et al. *Plasmodium falciparum* normocyte binding protein (PfNBP-1) peptides bind specifically to human erythrocytes. Peptides 2003;24:1007–14.
[70] Vera-Bravo R, Torres E, Valbuena JJ, Ocampo M, Rodríguez LE, Puentes A, et al. Characterising *Mycobacterium tuberculosis* Rv1510c protein and determining its sequences that specifically bind to two target cell lines. Biochem Biophys Res Commun 2005;332:771–81.
[71] Vizcaino C, Restrepo-Montoya D, Rodriguez D, Nino LF, Ocampo M, Vanegas M, et al. Computational prediction and experimental assessment of secreted/surface proteins from *Mycobacterium tuberculosis* H37Rv. PLoS Comput Biol 2010;6:e1000824.
[72] Wagner B, Fattorini L, Wagner M, Jin SH, Stracke R, Amicosante G, et al. Antigenic properties and immunoelectron microscopic localization of *Mycobacterium fortuitum* beta-lactamase. Antimicrob Agents Chemother 1995;39:739–45.
[73] Wagner D, Maser J, Lai B, Cai Z, Barry ICE, Bentrup KH, et al. Elemental analysis of *Mycobacterium avium*, *Mycobacterium tuberculosis* and *Mycobacterium smegmatis* containing phagosomes indicates pathogen-induced microenvironments within the host cell's endosomal system. J Immunol 2005:1491–500.
[74] Weiland GA, Molinoff PB. Quantitative analysis of drug-receptor interactions: I. Determination of kinetic and equilibrium properties. Life Sci 1981;29:313–30.
[75] Weldingh K, Rosenkrands I, Jacobsen S, Birk Rasmussen P, Elhay MJ, Andersen P. Two-dimensional electrophoresis for analysis of *Mycobacterium tuberculosis* culture filtrate and purification and characterization of six novel proteins. Infect Immun 1998;66:3492–500.
[76] WHO. Global tuberculosis control 2009 epidemiology strategy financing. Geneva: World Health Organization; 2009.
[77] Win J, Morgan W, Bos J, Krasileva KV, Cano LM, Chaparro-Garcia A, et al. Adaptive evolution has targeted the C-terminal domain of the RXLR effectors of plant pathogenic oomycetes. Plant Cell 2007;19:2349–69.
[78] World Health Organization. What is DOTS? A guide to understanding the WHO-recommended TB control strategy known as DOTS. Geneva: World Health Organization; 1999.
[79] Xiong Y, Chalmers MJ, Gao FP, Cross TA, Marshall AG. Identification of *Mycobacterium tuberculosis* H37Rv integral membrane proteins by one-dimensional gel electrophoresis and liquid chromatography electrospray ionization tandem mass spectrometry. J Proteome Res 2005;4:855–61.
[80] Xu S, Cooper A, Sturgill-Koszycki S, van Heyningen T, Chatterjee D, Orme I, et al. Intracellular trafficking in *Mycobacterium tuberculosis* and *Mycobacterium avium*-infected macrophages. J Immunol 1994;153:2568–78.
[81] Yamamura HY, Enna SJ, Kuhar M. Neurotransmitter receptor binding. New York: Raven Press; 1978.